

B QUARK PHYSICS : RECENT RESULTS FROM UA1

Jeffrey B. Gronberg
University of California, Los Angeles
 405 Hilgard Ave, Los Angeles, CA, 90024, USA
 for the UA1 Collaboration,* CERN
 Geneva, Switzerland



ABSTRACT

We present the results of the b -quark analysis of the UA1 '88 and '89 physics runs ($4.7pb^{-1}$). We measure inclusive b -quark production over a wide range of p_T^b and find good agreement with $O(\alpha_s^3)$ predictions over 5 orders of magnitude. The rate of $B^0\bar{B}^0$ mixing is measured to be $\chi = 0.145^{+0.040}_{-0.036}$. We use measurements of B_d^0 mixing from ARGUS and CLEO to determine the rate of B_s^0 mixing in our data to be $\chi_s = 0.50 \pm 0.20$. Finally, we present the results of a search for the rare B -hadron decays $B^0 \rightarrow \mu^+\mu^-$, $B \rightarrow \mu^+\mu^-X$, $B_d \rightarrow \mu^+\mu^-K^0$. The new results allow us to put a limit on $M_{top} < 400 GeV/c^2$ at 90% C.L.

*Aachen - Amsterdam (NIKHEF) - Annecy (LAPP) - Birmingham - Boston - CERN - Helsinki - Kiel - Imperial College, London - Queen Mary College, London - Madrid (CIEMAT) - MIT - Padua - Paris (College de France) - Rome - Rutherford Appleton Lab - Saclay (CEN) - UCLA - Vienna Collaboration

1 Introduction

Presuming a $b\bar{b}$ production cross section of $10\mu b$ at $\sqrt{s} = 630\text{ GeV}$, there should be $\sim 5 \cdot 10^7$ $b\bar{b}$ pairs in our sample of 4.7 pb^{-1} . The potential for studying $b\bar{b}$ physics with this sample is good. We observe b -quarks by their decays into high p_t muons. A detailed description of the detector has been given in previous papers.¹ Detailed discussion of the work presented here has been published elsewhere.^{2, 3, 4}

2 b-Quark Production

We have used four independent data samples to measure b -quark production:

- Muon-Jet - an inclusive single muon + jet sample
- $B \rightarrow J/\psi$ - a sample of high p_t J/ψ 's from decays of B -Hadrons
- Low-Mass Dimuons - a dimuon sample with the invariant mass of the two muons ($M_{\mu\mu}$) less than $6\text{ GeV}/c^2$
- High-Mass Dimuons - a dimuon sample with $6 < M_{\mu\mu} < 35\text{ GeV}/c^2$

For each sample we measure a muon-level cross section $\sigma(p\bar{p} \rightarrow b \rightarrow \mu's)$. We then use a Monte Carlo simulation of the $b \rightarrow \mu$ process to extrapolate to the b -level cross section. Since we have information only on p_t^b and not p_t^b , we choose to quote a p_t^b dependent cross section for each sample

$$\sigma(p\bar{p} \rightarrow bX; p_t^b > p_t^{\text{min}}, |y_b| < 1.5) = \int_{-1.5}^{1.5} dy_b \int_{p_t^{\text{min}}}^{\infty} dp_t^b \frac{d^2\sigma(p\bar{p} \rightarrow bX)}{dy_b dp_t^b} \quad (1)$$

where p_t^{min} is chosen such that of all Monte Carlo b -quark events which pass the cuts for the sample, 90% have $p_t^b > p_t^{\text{min}}$. The b -level cross section can then be compared with the recently calculated $O(\alpha_s^3)$ QCD prediction.⁵

The major sources of systematic error on the cross section are the luminosity (8%), acceptance ($\sim 10\%$) and p_t^b resolution (2% at $10\text{ GeV}/c$ to 50% at $40\text{ GeV}/c$). Furthermore the Muon-Jet sample has a jet energy scale error (12%). The extrapolation from muon level to b -level cross section includes three more systematic errors. The uncertainties due to the b -quark fragmentation function, the semi-leptonic branching ratio and decay kinematics of the B -hadron, and the shape of the b -quark p_t spectrum in our Monte Carlo.⁶

We have used recent ALEPH data for $Z^0 \rightarrow b\bar{b}$ ⁷ (see Figure 1) to tune the ε_b parameter in the Peterson fragmentation function.⁸ We find $\varepsilon_b \sim 0.02 \pm 0.01$ which leads to a 6% error in the cross section. We have averaged the recent results of ARGUS and CLEO⁹ to determine the semileptonic branching fraction of B -hadrons $Br(b \rightarrow \mu) = 10.2\% \pm 1.0\%$. We have also checked that the V-A, spectator model used in ISAJET for semileptonic B -meson decays gives good agreement with recent $\Upsilon(4S)$ measurements from ARGUS and CLEO¹⁰. For the Low-Mass Dimuons there is uncertainty on the mixture of charmed hadrons produced in B -decays. We include a 20% error on the average $c \rightarrow \mu$ branching ratio to take this into account. Finally we assume a 20% uncertainty on the ISAJET shape of $d\sigma/dp_t^b$. Overall, the shape agrees well with the $O(\alpha_s^3)$ prediction of Nason, *et al.*⁵

2.1 The Muon-Jet Sample

The Muon-Jet data sample comes from single muon data ($p_t^\mu > 10 \text{ GeV}/c$) with an accompanying jet ($E_t^{\text{jet}} > 10 \text{ GeV}$). The jet requirement reduces W/Z decay background.

Events from b -quarks can be separated from background on a statistical basis by using the quantity $(p_t^{\text{rel}})^*$, since the distribution of p_t^{rel} peaks higher with higher hadron mass. Using this technique we fit a $b\bar{b}$ fraction of $0.33 \pm 0.03(\text{stat}) \pm 0.03(\text{syst})$ in the Muon-Jet data. The cross section, separated into bins of different p_t^μ , is given in Table 1.

2.2 The $B \rightarrow J/\psi$ Sample

High p_t J/ψ 's are produced at the collider primarily through two processes: either directly via gluon-gluon fusion to χ states which tend to give Isolated J/ψ 's, or through the decay of B -Hadrons where the J/ψ 's are accompanied by other B decay products and hence are Non-Isolated.

$$\begin{array}{ccc}
 gg \rightarrow \chi g & & gg \rightarrow b\bar{b} \rightarrow BX \\
 \hookrightarrow J/\psi \gamma & & \hookrightarrow J/\psi X \\
 \hookrightarrow \mu^+ \mu^- & & \hookrightarrow \mu^+ \mu^-
 \end{array}$$

The difference in the Monte Carlo isolation distributions for these two processes is used to separate them on a statistical basis. We find the fraction of $B \rightarrow J/\psi$ events in the sample to be $0.31 \pm 0.02(\text{stat}) \pm 0.12(\text{syst})$ where the systematic error is primarily from the uncertainty in the fragmentation process.

We use $Br(b \rightarrow J/\psi) = (1.12 \pm 0.18)\%$, $Br(J/\psi \rightarrow \mu^+ \mu^-) = (6.9 \pm 0.9)\%$ and the measured J/ψ production cross section to find the muon level and b -quark level cross sections (see Table 1).

2.3 The Low-Mass Dimuon Sample

The Low-Mass Dimuon sample ($p_t^\mu > 3 \text{ GeV}/c$, $M_{\mu\mu} < 6 \text{ GeV}/c^2$) is chosen to be sensitive to b -chain decays.

$$\begin{array}{ccc}
 b \rightarrow c\mu\nu & & \\
 \hookrightarrow s\mu\nu & &
 \end{array}$$

For this sample we determine the fraction of b -quarks by a fit to the dimuon mass distribution ($M_{\mu\mu}$). We separate out low mass mesons, decay background, Drell-Yan, and heavy flavor decays. The result of the fit is a b -fraction of 0.14 ± 0.04 .

From this fraction we estimate the cross-section for muons from b -chain decays, $\sigma(p\bar{p} \rightarrow b \rightarrow \mu\mu X; p_t^\mu > 3 \text{ GeV}/c, |\eta_\mu| < 1.5, M_{\mu\mu} < 6 \text{ GeV}/c^2)$ and extrapolate to b -quark and hadron-level results (see Table 1).

2.4 The High-Mass Dimuon Sample

The cut $M_{\mu\mu} > 6 \text{ GeV}/c^2$ insures that the muons in this sample come from separate b -quarks and excludes low mass mesons. We also cut on $M_{\mu\mu} < 35 \text{ GeV}/c^2$ in order to eliminate

* p_t^{rel} is defined as the momentum of the muon transverse to the jet axis.

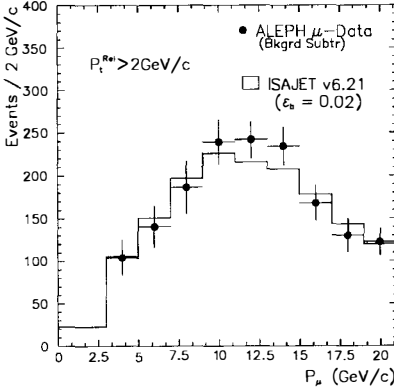


Figure 1: Comparison of ALEPH data for $Z \rightarrow b\bar{b} \rightarrow \mu$ (background subtracted) with the prediction of ISAJET for the same process using $\epsilon_b = 0.02$

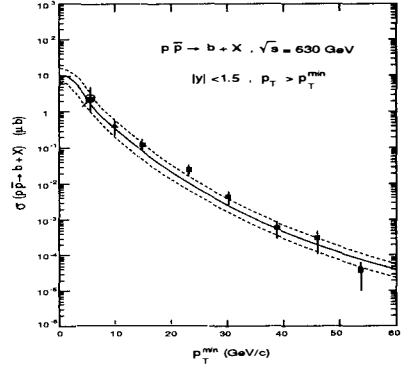


Figure 2: The b -quark cross-section for $|y_b| < 1.5$ versus p_T^{min} . The solid curve is the $O(\alpha_s^3)$ prediction of Nason *et al*. The dashed curve is the error band on this prediction from varying m_b , μ , and Λ

$Z \rightarrow \mu^+ \mu^-$ decays. As in the Muon-Jet sample we use p_t^{*el} to separate $b\bar{b}$ events from backgrounds. We find fractions of $b\bar{b}$ events in the like and unlike-sign data of $0.63 \pm 0.08(stat) \pm 0.01(syst)$ and $0.55 \pm 0.04(stat) \pm 0.01(syst)$ respectively.

Combining the like and unlike-sign results we find a cross-section for dimuons from different b -quarks, $\sigma(p\bar{p} \rightarrow b\bar{b} \rightarrow \mu\mu X; p_t^\mu > 3 \text{ GeV}/c, |\eta_\mu| < 1.5, 6 < M_{\mu\mu} < 35 \text{ GeV}/c^2)$ which is extrapolated to a b -quark and hadron-level result (see Table 1).

2.5 Total Cross-Sections

In Figure 2 we plot the inclusive b -level cross-section as a function of p_t^{min} for the quark measurements of each sample. Also shown on this plot is the prediction of Nason, *et al* for $d\sigma/dp_t^{min}$. The error bands on the prediction are due to uncertainties on the renormalization scale μ , the b -quark mass, and the mass scale Λ .

Using the Nason curve normalized to our data to extrapolate back to $p_t^{min} = 0$, we find the total inclusive b -quark production cross-section $\sigma(p\bar{p} \rightarrow bX; |y_b| < 1.5) = 12.8_{-5.4}^{+7} \mu b$. This agrees with the absolute prediction of the theory $(10.2_{-3.8}^{+5.8} \mu b)$.

3 $B^0 \bar{B}^0$ Mixing

Oscillation of neutral particles into their anti-particles is allowed in the Standard Model by 2nd order diagrams. We define a quantity χ that is the probability that a B^0 meson will oscillate into it's anti-particle before decaying.

$$\chi = \frac{BR(B^0 \rightarrow \bar{B}^0 \rightarrow \mu^- \nu_\mu X)}{BR(B^0 \rightarrow \mu^\pm \nu_\mu X)}$$

Since different CKM matrix elements appear in the theoretical calculations for B_d^0 and B_s^0 , χ_d and χ_s will not be identical. At the $Spp\bar{p}S$ collider energies a mixture of both types of B^0

Table 1: Results of muon-level and b-level cross-section calculations

Sample	Muon		<i>b</i> -Quark	
	p_t^μ Range [GeV/c]	$\sigma(\mu - level)$ [nb]	p_t^{min} [GeV/c]	$\sigma(b - level)$ [nb]
$B \rightarrow J/\psi$	$p_t^{J/\psi} > 5, y < 2$	1.92 ± 0.80	6.0	2360 ± 1215
High-Mass Dimuons	> 3	2.12 ± 0.39	6.0	2660 ± 1330
Low-Mass Dimuons	> 3	0.31 ± 0.08	10	390 ± 170
Muon-Jet	10-15	1283 ± 269	15	120 ± 38
	15-20	180 ± 140	23	24 ± 8
	20-25	24.3 ± 6.5	30	4.1 ± 1.4
	25-30	3.2 ± 1.4	39	0.55 ± 0.3
	30-35	1.1 ± 0.6	46	0.32 ± 0.2
	35-40	0.14 ± 0.09	54	0.04 ± 0.03

mesons are produced, thus our measured χ will be a linear combination of χ_d and χ_s .

3.1 Data sample

We measure mixing in the high mass dimuon sample. We use a cut on $M_{\mu\mu} > 6\text{GeV}/c^2$ to remove dimuons from low-mass mesons and from b-chain decays. The muons are also required to be non-isolated in order to remove Drell-Yan and Υ events. Since the flavor quantum number of the decaying meson determines the sign of the muon, in $b\bar{b}$ events with no mixing we expect the two muons to be unlike-sign. In the presence of mixing there is a probability that one of the mesons will oscillate before decaying. In this case a like-sign event would be observed. From this we can see that it is possible to measure mixing by comparing the number

Table 2: Probability of $b\bar{b}$ events producing unlike-sign and like-sign dimuons

$p\bar{p} \rightarrow b\bar{b} \rightarrow B^0\bar{B}^0 \rightarrow \mu^- \nu_\mu X$ $\hookrightarrow \mu^+ \nu_\mu X$	$\chi^2 + (1 - \chi)^2$	unlike-sign
$p\bar{p} \rightarrow b\bar{b} \rightarrow B^0\bar{B}^0 \rightarrow \mu^- \nu_\mu X$ $\hookrightarrow \bar{B}^0 \rightarrow \mu^- \nu_\mu X$	$2\chi(1 - \chi)$	like-sign

of unlike-sign and like-sign dimuon events in the data to the monte carlo prediction.

3.2 Separation of $b\bar{b}$ events from background

The dimuon events are produced by the sources listed below; only the first two yield information on $B^0\bar{B}^0$ mixing.

- 1st generation $b\bar{b}$ – These are events in which both B-mesons decay directly into muons.
- 2nd generation $b\bar{b}$ – These are events in which one B-meson decays directly into a muon while the other decays to a muon via a C-Meson.
- $c\bar{c}$ – Events in which both C-mesons decay directly into muons.
- Decay Background – Dimuon events where one or both muons come from decays in flight of π or K mesons.
- Drell-Yan – $p\bar{p} \rightarrow \gamma, Z \rightarrow \mu^+ \mu^-$
- Υ – $p\bar{p} \rightarrow \Upsilon \rightarrow \mu^+ \mu^-$

We separate the $b\bar{b}$ events from background events on a statistical basis by fitting Monte Carlo p_i^{rel} distributions for each process to the data. Each distribution is made by fitting a parameterized curve to the Monte Carlo events. The p_i^{rel} distributions of the $b\bar{b}$ events peak at a higher value than the distributions for Decay background and $c\bar{c}$. The muons in each dimuon event are separated into muons of higher and lower p_t , and p_i^{rel} distributions are made for each ($p_i^{rel} hi$ and $p_i^{rel} lo$ respectively). The data, separated into unlike-sign and like-sign samples, is shown in Figure 3.

3.3 Mixing measurements and B_s^0 limits

The minimum of the fit occurs at $\chi = 0.145_{-0.036}^{+0.040}$, where the uncertainty derived from the fit includes both statistical and systematic uncertainties. The $\chi = 0.0$ region is excluded at about the 4σ level. The systematic uncertainties are included in the fit as variables and allowed to vary within a Gaussian constraint. By fixing these variables to their best fit value and observing the decrease in the total error on χ the error can be separated into statistical and systematic parts. In order to separate them we assume a symmetrical error of ± 0.038 on χ .

New result: $\chi = 0.145 \pm 0.035(stat) \pm 0.014(syst)$

Previous result: $\chi = 0.158 \pm 0.052(stat) \pm 0.026(syst)$

Combining these results assuming fully correlated systematic errors we get

Combined result: $\chi = 0.148 \pm 0.029(stat) \pm 0.017(syst)$

The measured value of χ is a combination of χ_d and χ_s , namely $\chi = f_{dd}\chi_d + f_{ss}\chi_s$ where f_{qq} is the probability of a b-quark forming a $b\bar{q}$ meson during hadronization. We use $f_{dd} = 0.36$ and $f_{ss} = 0.18$.¹¹ By combining the UA1 measurement of χ with a measurement of χ_d from ARGUS and CLEO¹² ($\chi_d = 0.162 \pm 0.039$) we can determine χ_s as shown in Figure 4. When these two measurements are combined we determine $\chi_s = 0.50 \pm 0.20$. The $\pm 1\sigma$ region extends into a non-physical region. In order to set a one dimensional limit on χ_s we cut away the non-physical region and renormalize the remaining probability density to one. We find $\chi_s > 0.17(0.12)$ at 90% (95%)C.L. and we show the two dimensional 90% and 95% C.L. ellipses in Figure 5 We can also include in the fit the measurements of χ from Aleph¹³ ($\chi = 0.132 \pm 0.027$) and L3¹⁴ ($\chi = 0.178 \pm 0.045$). Repeating the analysis including the LEP measurements we find $\chi_s = 0.53 \pm 0.15$ and $\chi_s > 0.27(0.23)$ at 90% (95%)C.L.

4 Rare B-Decays

We present branching ratio limits for three different rare B-hadron decay modes: $B^0 \rightarrow \mu^+ \mu^-$, $B \rightarrow \mu^+ \mu^- X$, $B_d \rightarrow \mu^+ \mu^- K^0$. These decays measure the relative strength of Flavor Changing Neutral Currents (FCNC) which are forbidden by the Standard Model at the tree-level, but expected due to loop diagrams. The presence of these quark loops make the branching ratios sensitive to the top-quark mass. In Table 3 we compare several theoretical predictions with our measurements and results from other experiments.

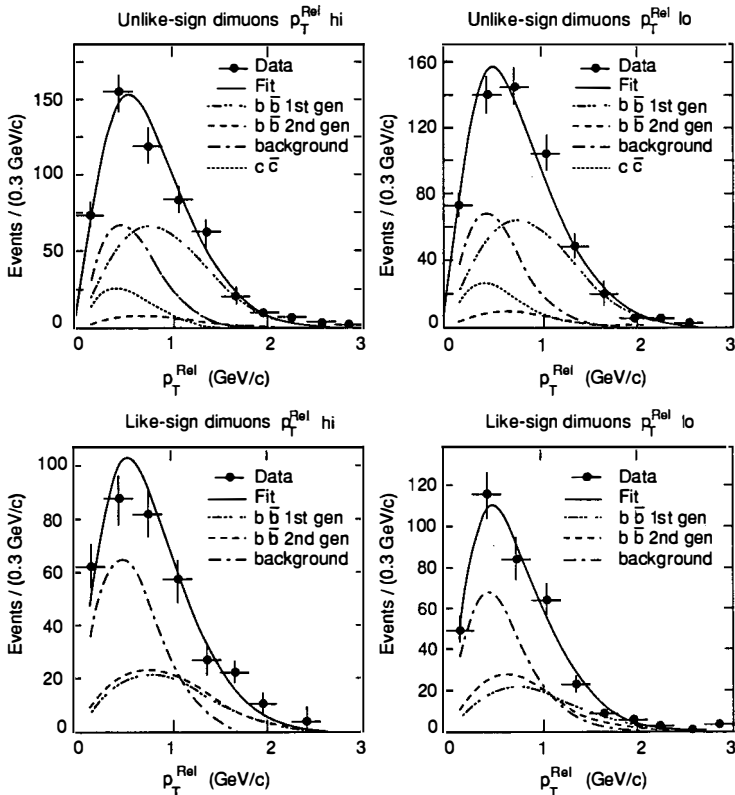


Figure 3: p_T^{rel} for unlike-sign and like-sign events with the fitted curves

4.1 Branching Ratio Limits

The data sample for the $B^0 \rightarrow \mu^+ \mu^-$ and $B \rightarrow \mu^+ \mu^- X$ searches is unlike-sign dimuons of $p_T^{\mu\mu} > 7 \text{ GeV}/c^2$. The search region in dimuon mass for the $B^0 \rightarrow \mu^+ \mu^-$ decay, $5.1 < M_{\mu\mu} < 5.5 \text{ GeV}/c^2$, is centered on the B_d mass with a width given by the detector dimuon mass resolution, $\sim 200 \text{ MeV}/c^2$. For $B \rightarrow \mu^+ \mu^- X$ decays we choose a mass region for $B \rightarrow \mu^+ \mu^- X$ candidates of $3.9 < M_{\mu\mu} < 4.4 \text{ GeV}/c^2$, to avoid interference from J/ψ and ψ' decays.¹⁷

In these analyses we use $M(B_d) = 5.28 \text{ GeV}/c^2$,¹⁸ and assume $M(B_s) = 5.38 \text{ GeV}/c^2$. The B -hadronization ratio is assumed to be $B^\pm : B_d : B_s : B\text{-baryon} = 36 : 36 : 18 : 10$.

A plot of the data in and around the regions of interest is shown in Figure 6. We determine the background for our searches by a fit to the data outside of the search regions. This fit contains Gaussians centered at the J/ψ and ψ' masses and a term linear in $M_{\mu\mu}$. As can be seen from Figure 6 there are no significant excesses of events in either search region. This allows us to place upper limits on these branching ratios which are given in Table 3.

In the search for $B_d \rightarrow \mu^+ \mu^- K^{*0}$ we relax the $p_T^{\mu\mu}$ cut since we ultimately demand a

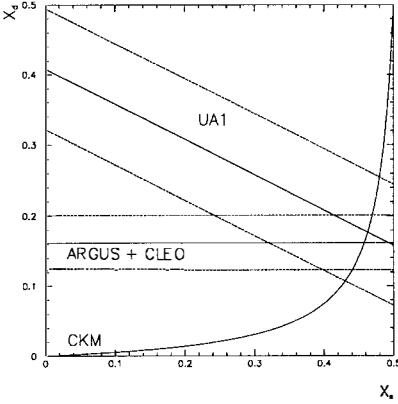


Figure 4: Relationship of χ_d versus χ_s for the UA1 combined result. The central value and $\pm 1\sigma$ lines are drawn. The combined ARGUS and CLEO results for χ_d are also drawn.

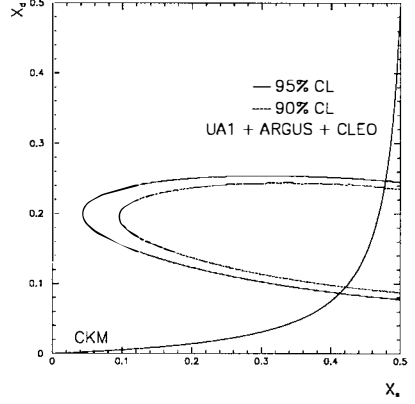


Figure 5: Confidence ellipses for χ_d versus χ_s using the UA1 measurement and the ARGUS and CLEO measurement.

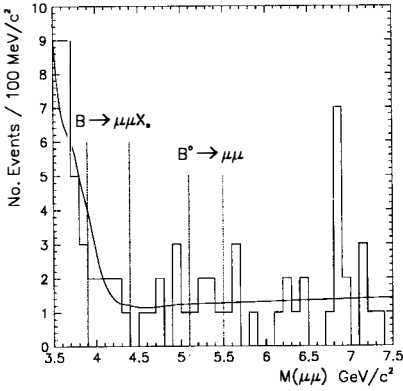


Figure 6: The dimuon invariant mass distribution in the $B^0 \rightarrow \mu^+\mu^-$ and $B \rightarrow \mu^+\mu^-X$ search regions. The solid line represents the fit to the background

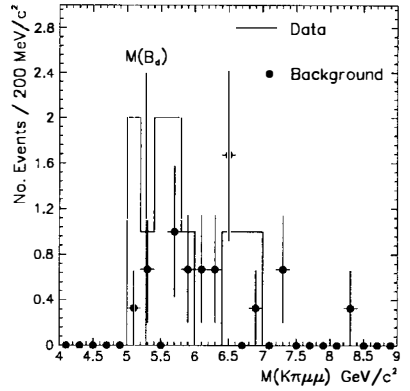


Figure 7: The $K\pi\mu\mu$ mass distribution for events near the $B_d \rightarrow \mu^+\mu^-K^{0*}$ search region with background estimate

Table 3: Predicted branching ratios (for $100 < M_{top} < 200 \text{ GeV}/c^2$) and experimental limits for rare B -decays

Process	Branching Ratios		
	Theoretical Prediction	UA1 Limit (90% C.L.)	Other Limits (90% C.L.)
$B_{s,d} \rightarrow \mu^+ \mu^-$ $B_s \rightarrow \mu^+ \mu^-$ $B_d \rightarrow \mu^+ \mu^-$	$4 \cdot 10^{-10} - 4 \cdot 10^{-9}$ ¹⁶	$8.3 \cdot 10^{-6}$ $2.5 \cdot 10^{-5}$ $1.2 \cdot 10^{-5}$	$5 \cdot 10^{-5}$ ARGUS ¹⁹ CLEO ²⁰ $3.2 \cdot 10^{-6}$ CDF ²¹
$B \rightarrow \mu^+ \mu^- X$	$3 \cdot 10^{-5} - 7 \cdot 10^{-5}$ ²²	$5 \cdot 10^{-5}$	$2.4 \cdot 10^{-3}$ CLEO ²³
$B_d \rightarrow \mu^+ \mu^- K^{0*}$	$2 \cdot 10^{-7} - 8 \cdot 10^{-7}$ ¹⁵	$1.1 \cdot 10^{-5}$	$1.9 \cdot 10^{-4}$ CLEO ²⁰

$K^{0*} \rightarrow K^+ \pi^-$ candidate in the event. The background to this sample is estimated by loosening the cuts on the $K\pi$ system.

The data and background estimation are plotted in Figure 7. Again we see no significant excess of data events in a region of $\pm 200 \text{ MeV}/c^2$ around the B_d mass. The branching ratio upper limit we derive is given in Table 3.

4.2 Top Mass Limit

Grigjanis *et al* ²² have calculated the branching ratio $\text{Br}(b \rightarrow l^+ l^- s)$ as a function of M_{top} . This quark level calculation can be compared to our measured $\text{Br}(B \rightarrow \mu^+ \mu^- X)$ upper limit. Comparing the calculation with our upper limit we find $M_{top} < 400 \text{ GeV}/c^2$ at 90% C.L. This limit is independent of the possible decay modes of the top-quark.

5 Conclusions

We have studied several aspects of heavy quark physics at UA1 ranging from production to decay modes and mixing. We find excellent agreement between our measurements of b -quark production and $O(\alpha_s^3)$ QCD predictions over a wide range of transverse momentum. We find B_s^0 mixing to be maximal, consistent with Standard Model predictions, and exclude the region of zero mixing. We have also improved branching ratio limits for loop-induced B -hadron decays by an order of magnitude over previous results from e^+e^- experiments.

Acknowledgements

I would like to thank all of my colleagues at UA1 who made this work possible.

References

- [1] C. Albajar *et al* (UA1 Collab.), *Z. Phys.* **C48** (1990) 1.
- [2] C. Albajar *et al* (UA1 Collab.), *CERN-PPE/90-155*.
- [3] C. Albajar *et al* (UA1 Collab.), *CERN-PPE/91-55*.
- [4] C. Albajar *et al* (UA1 Collab.), *CERN-PPE/91-54*.
- [5] P. Nason, S. Dawson, R.K. Ellis, *Nucl. Phys.* **B303** (1988) 607, *Nucl. Phys.* **B327** (1989) 49.
W. Beenakker *et al*, *DESY 90-064*, *ITP-SB-90-46* (1990).
- [6] F. Paige, S.D. Protopopescu, *BNL-38034* (1986).
- [7] R. Johnson, talk given at *XXV Int. Conf. on High Energy Physics, Singapore 1990*.
- [8] C. Peterson *et al*, *Phys. Rev.* **D27** (1986) 105.
- [9] H. Albrecht *et al* (ARGUS Collab.), *DESY 90-088* (1990).
R. Fulton *et al* (CLEO Collab.), *Phys. Rev. Lett.* **64** (1990) 16.
- [10] M. Danilov (for the ARGUS Collab.), *DESY 89-147* (1989).
M. Artuso *et al* (CLEO Collab.), *Phys. Lett.* **62** (1989) 2233.
- [11] M. Banner *et al* (UA2 Collab.), *Phys. Lett.* **B122** (1983) 322;
A. Breakstone *et al*, *Phys. Lett.* **B135** (1984) 510;
G.J. Alner *et al* (UA5 Collab.), *Nucl. Phys.* **B258** (1985) 505.
- [12] H. Albrecht *et al* (ARGUS Collab.), *Phys. Lett.* **B192** (1987) 246;
A. Bean *et al* (CLEO Collab.), *Phys. Rev. Lett.* **58** (1987) 183.
- [13] D. Decamp *et al* (ALEPH Collab.), *CERN-PPE 90-194*, submitted to *Phys. Lett. B*.
- [14] B. Adeva *et al* (L3 Collab.), *L3 preprint #20*, submitted to *Phys. Lett. B*.
- [15] W. Jaus and D. Wyler, *Phys. Rev.* **D41** (1990) 3705.
- [16] J.L. Hewett *et al*, *Phys. Rev.* **D39** (1989) 250.
- [17] C.S. Lim *et al*, *Phys. Lett.* **B218** (1989) 343.
- [18] Particle Data Group, *Phys. Lett.* **B239** (1990).
- [19] H. Albrecht *et al* (ARGUS Collab.), *Phys. Lett.* **B199** (1987) 451.
- [20] P. Avery *et al* (CLEO Collab.), *Phys. Lett.* **B223** (1989) 470.
- [21] T.F. Rohaly, talk given at *XXV Int. Conf. on High Energy Physics, Singapore 1990*.
- [22] R. Grigjanis *et al*, *UTPT-89-32* (1989).
P. O'Donnell, private communications.
- [23] A. Bean *et al* (CLEO Collab.), *Phys. Rev.* **D35** (1987) 3533.
- [24] E.W.N. Glover, A.D. Martin, W.J. Stirling, *Z. Phys.* **C38** (1988) 473, and private communications with E.W.N. Glover.